

Cell-Permeable  $\beta^3$ -Peptide Inhibitors of p53/hDM2 ComplexationElizabeth A. Harker and Alanna Schepartz\*<sup>[a]</sup>

Properly designed  $\beta^3$ -peptides can inhibit protein–protein interactions, in large part because of their ability to reproduce the side chain presentation of one face of an  $\alpha$ -helix.<sup>[1–5]</sup> This activity, combined with virtually complete resistance to proteolysis,<sup>[1,6]</sup> has led to the prediction that  $\beta^3$ -peptides could effectively modulate biological pathways. This promise has been limited by a genuine physical barrier—the plasma membrane—which most  $\beta^3$ -peptides cannot traverse. A general strategy to increase cellular uptake of  $\beta^3$ -peptides would accelerate the widespread application of these molecules as tools or therapeutics. Although polyarginine tags can improve cell uptake of peptides and proteins,<sup>[7,8]</sup> they can also increase toxicity<sup>[8]</sup> and diminish protein stability.<sup>[9]</sup> Moreover, in the context of a  $\beta^3$ -peptide dodecamer, a polyarginine tag adds considerable molecular mass.

We reported recently that miniature proteins<sup>[10,11]</sup> cross the plasma membrane of living mammalian cells and localize in the cytosol when a minimal cationic motif is embedded within their folded structure.<sup>[12]</sup> Here we report that an analogous approach increases the cell permeability of  $\beta^3$ -peptide inhibitors of hDM2/p53 complexation. The molecules we describe thus serve as a starting point for the combinatorial identification of  $\beta^3$ -peptides with improved cell uptake and unique biological function. We note that others have previously described cell-penetrating  $\beta^3$ -peptides containing multiple arginine side chains,<sup>[13–15]</sup> however, with the exception of a  $\beta^3$ -peptide based on the Tat translocation sequence,<sup>[14]</sup> these studies all involved  $\beta^3$ -peptide homopolymers, none of which possessed biological function.

Our work began with two previously reported  $3_{14}$ -helical

$\beta^3$ -peptides with high affinity for hDM2,  $\beta^3$ -8 and  $\beta^3$ -12,<sup>[5,16]</sup> which both upregulate p53 activity when internalized with a commercial transduction reagent (BioPORTER<sup>®</sup>, Sigma).<sup>[17]</sup> The  $3_{14}$ -helical structure of these molecules presents three distinct faces: an epitope face containing side chains that interact directly with hDM2; a salt bridge face that promotes water solubility and secondary structure; and a structural face that can be varied to fine-tune the helix. We began by asking whether these two molecules would become cell permeable when two to three  $\beta^3$ -homoarginine ( $\beta^3$ hR) residues were embedded within either the “structural” (strategy 1) or “salt bridge” face (strategy 2; Figure 1). As negative controls we synthesized variants of  $\beta^3$ -3, a well-folded  $\beta^3$ -peptide that binds poorly to hDM2,<sup>[4]</sup> and  $\beta$ NEG, which lacks an hDM2 recognition epitope. As positive controls we synthesized variants of  $\beta^3$ -12 and

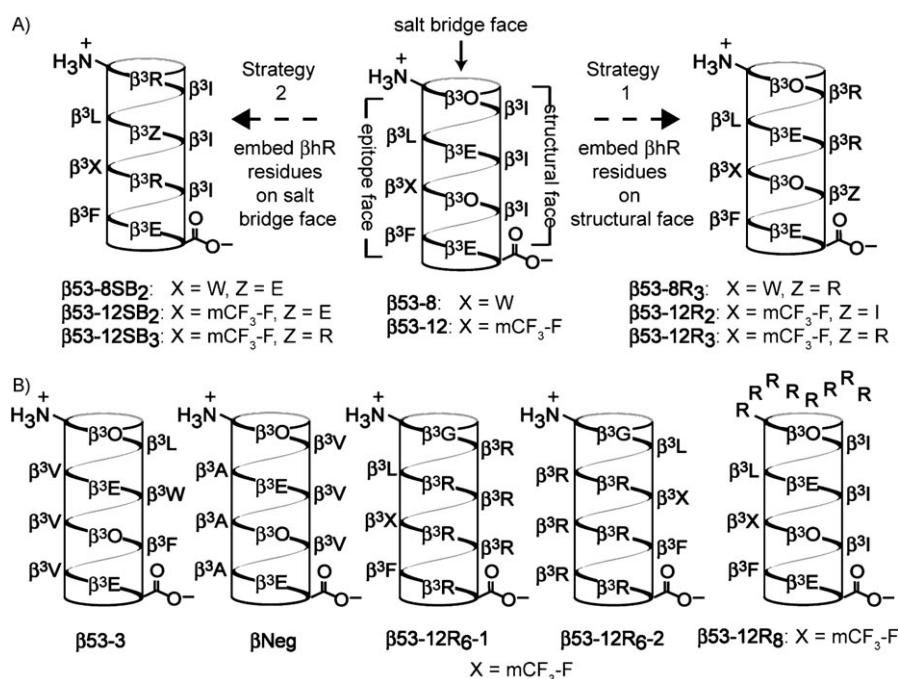


**Figure 1.** A) Two strategies to increase the cell permeability of  $\beta^3$ -peptides that bind hDM2. In strategy 1,  $\beta^3$ -homoarginine residues are embedded into the  $\beta^3$ -peptide structural face, while in strategy 2 they are embedded into the salt bridge face. B) Helical net representation of  $\beta^3$ -peptides studied as controls.  $\beta^3$ -homoamino acids are identified by the one-letter-code corresponding to the analogous  $\beta^3$ -amino acid where CF<sub>3</sub>-F denotes 3-trifluoromethylphenylalanine.

$\beta^3$ -3 containing an N-terminal Arg<sub>8</sub> tag ( $\beta^3$ -12R<sub>8</sub> and  $\beta^3$ -3R<sub>8</sub>, respectively).

We first compared strategies 1 and 2 with respect to their ability to maintain  $3_{14}$ -helical structure. The circular dichroism (CD) signature of a  $3_{14}$ -helix, in particular the ellipticity minimum at  $\sim 214$  nm, provides a qualitative measure of secondary structure.<sup>[2,18]</sup> The data indicate that  $\beta^3$ -peptides with  $\beta^3$ -homo-

[a] E. A. Harker, Prof. A. Schepartz  
 Department of Chemistry, Yale University  
 225 Prospect Street, New Haven, CT 06520 (USA)  
 Fax: (+1) 203-432-3486  
 E-mail: alanna.schepartz@yale.edu

Supporting information for this article is available on the WWW under <http://dx.doi.org/10.1002/cbic.200900049>.

arginine ( $\beta^3$ hR) residues embedded on the salt bridge face ( $\beta 53-12SB_2$  and  $\beta 53-12SB_3$ , strategy 2) retain greater  $3_{14}$ -helical character than those modified on the structural face ( $\beta 53-12R_2$  and  $\beta 53-12R_3$ , strategy 1; Figure 2A and B). Not surpris-

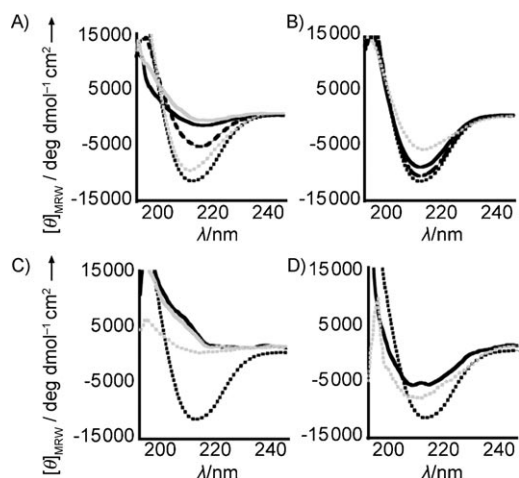


**Figure 2.** Circular dichroism spectra of  $\beta^3$ -peptides and controls (50  $\mu$ M) in Tris buffer (10 mM Tris, 100 mM NaCl, 0.01% Tween, pH 7.4).  $\beta 53-12$  ....; A)  $\beta 53-12R_2$  ----,  $\beta 53-12R_3$  —,  $\beta 53-8$  .....,  $\beta 53-8R_3$  —; B)  $\beta 53-12SB_2$  ----,  $\beta 53-12SB_3$  —,  $\beta 53-3SB_3$  .....,  $\beta 53-3SB_3$  —; C)  $\beta 53-12R_6-1$  —,  $\beta 53-12R_6-2$  —,  $\beta NEGR_6$  .....,  $\beta 53-12R_8$  —; D)  $\beta 53-12R_8$  —,  $\beta 53-3R_8$  .....,  $[\theta]_{MRW}$  = mean residue molar ellipticity.

ingly,  $\beta$ -peptides modified on both faces ( $\beta 53-12R_6-1$  and  $\beta 53-12R_6-2$ ) display virtually no  $3_{14}$ -helical character in aqueous solution (Figure 2C). Peptides modified with an  $\alpha$ -arginine tag ( $\beta 53-12R_8$  and  $\beta 53-3R_8$ ) retain structure but are not as  $3_{14}$ -helical as the parent peptides (Figure 2D).

Next, we compared the hDM2-affinities of the four sets of  $\beta^3$ -peptides using both direct and competition fluorescence polarization assays.<sup>[16]</sup> We found a direct correlation between  $3_{14}$ -helical structure and hDM2 affinity:  $\beta^3$ -peptides with  $\beta^3$ hR residues embedded within the salt bridge face ( $\beta 53-12SB_2$  and  $\beta 53-12SB_3$ ) displayed high  $3_{14}$ -helix levels by CD (Figure 2B) and bound hDM2 well ( $K_D = 41.7 \pm 4.23$  and  $120 \pm 2.00$ , respectively) (Figure 3B).<sup>[4,16]</sup> In contrast,  $\beta 53-8R_3$ ,  $\beta 53-12R_3$ ,  $\beta 53-12R_2$  and the highly cationic  $\beta 53-12R_6-1$  and  $\beta 53-12R_6-2$ , which were all less  $3_{14}$ -helical by CD, did not (Figure 3C). The  $\beta^3$ -peptides possessing the highest affinity for hDM2 in the direct binding assay ( $\beta 53-12SB_2$ ,  $\beta 53-12SB_3$ , and  $\beta 53-12R_8$ ) also inhibited the interaction between hDM2 and a p53-derived peptide (p53AD<sup>Flu</sup>) with  $IC_{50}$  values in the low micromolar range; their activity mimicked the activity of the parental  $\beta 53-12$  (Figure 3D).<sup>[16]</sup> These results indicate that at least in the context of hDM2 recognition, the most successful strategy for maintaining both hDM2 affinity and  $3_{14}$ -helical structure substitutes  $\beta^3$ hR for residues on the salt-bridging face, as replacement of other residues leads to a loss in both structure and affinity. Analysis of a computationally-generated model of  $\beta 53-12$  in complex with hDM2 suggests that the structural face may be in closer proximity to the hDM2 surface than the salt-bridge face; this provides one potential explanation for our observations.

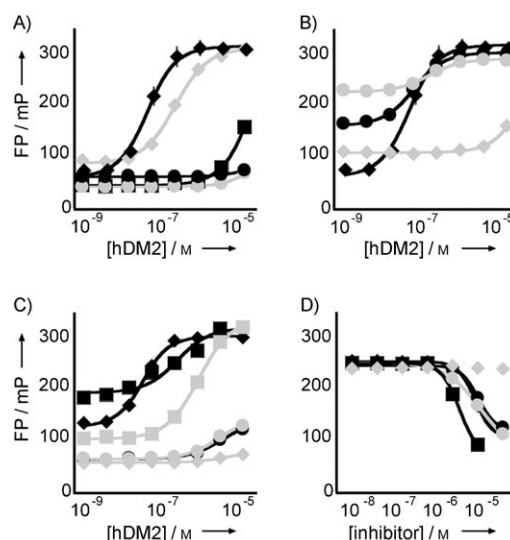


**Figure 3.** Plots illustrating direct (A–C) and competition (D) fluorescence polarization (FP) analysis of hDM2 binding by  $\beta^3$ -peptides studied herein. Equilibrium reactions were performed in Tris buffer (see legend to Figure 2). (A–C) Plots illustrating the observed polarization of the indicated fluorescently labeled  $\beta^3$ -peptide as a function of [hDM2]<sub>1–188</sub>.  $\beta 53-12$   $\blacklozenge$ ; A)  $\beta 53-12R_2$   $\blacksquare$ ,  $\beta 53-12R_3$   $\bullet$ ,  $\beta 53-8$   $\blacklozenge$ ,  $\beta 53-8R_3$   $\blacklozenge$ ; B)  $\beta 53-12SB_2$   $\bullet$ ,  $\beta 53-12SB_3$   $\bullet$ ,  $\beta 53-3SB_3$   $\blacklozenge$ ; C)  $\beta 53-12R_6-1$   $\bullet$ ,  $\beta 53-12R_6-2$   $\bullet$ ,  $\beta NEGR_6$   $\blacklozenge$ ,  $\beta 53-12R_8$   $\blacksquare$ ,  $\beta 53-3R_8$   $\blacksquare$ ; D) Plot illustrating the observed polarization of the p53AD<sub>15–31</sub><sup>Flu</sup> complex with hDM2<sub>1–188</sub> as a function of the concentration of unlabeled peptide shown:  $\beta 53-12$ ,  $\beta 53-12SB_2$ ,  $\beta 53-12SB_3$ ,  $\beta 53-12R_8$ , and  $\beta 53-3R_8$  (as above).

We also compared the four sets of  $\beta^3$ -peptides with respect to both cellular uptake and cytotoxicity (Figure 4). To assess cellular uptake we incubated approximately 500 000 HCT116 colon carcinoma cells with 10  $\mu$ M fluorescently tagged  $\beta^3$ -peptide for 1 h, washed the cells with PBS and trypsin, and quantified the resulting mean cellular fluorescence (MCF) using flow cytometry. Under these conditions, the uptake of the  $\alpha$ -pep-

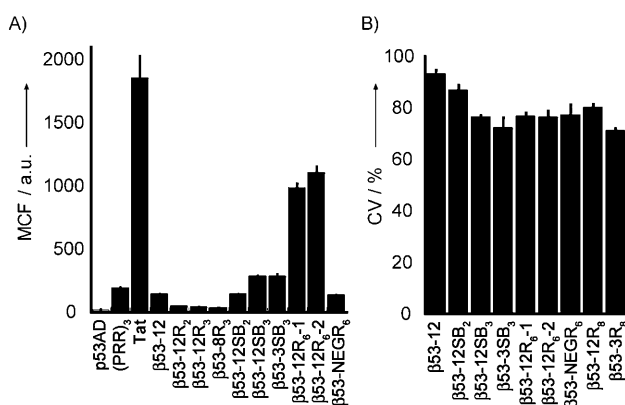


**Figure 4.** Uptake and viability of  $\beta^3$ -peptides studied herein. A) Flow cytometry analysis of  $\beta^3$ -peptide uptake by HCT116 cells after 1 h incubation. Mean cellular fluorescence (MCF) was calculated from the histogram of fluorescence intensity and was corrected for background cellular fluorescence by subtracting the geometric mean of cells treated with only PBS. Each value represents the average of three independent trials. Error bars represent the standard error. B) Viability of HCT116 cells upon incubation with the indicated  $\beta^3$ -peptide (10  $\mu$ M) for 8 h. Cell viability (CV) was measured using CellTiter-Blue<sup>TM</sup> as described in Experimental Methods. Each value represents the average of three independent trials. Error bars represent the standard error.

tide **p53AD<sup>Flu</sup>** was low as expected ( $MCF = 21.4 \pm 0.69$ ), whereas the validated cell-penetrating peptides (**PRR**)<sub>3</sub><sup>Flu</sup> and **Tat<sup>Flu</sup>** were taken up readily ( $MCF = 190 \pm 10.0$  and  $1850 \pm 182$  respectively).<sup>[12,19]</sup> None of the  $\beta^3$ -peptides containing  $\beta^3$ hR residues substituted on the structural face (strategy 1,  **$\beta 53-12R_2$** ,  **$\beta 53-12R_3$** ,  **$\beta 53-8R_3$** ) were taken up efficiently ( $MCF < 50$ ), perhaps because they possess only limited  $3_{14}$ -helical structure.<sup>[15]</sup> In contrast, all of the  $\beta^3$ -peptides with  $\beta^3$ hR residues substituted on the salt bridge face (strategy 2,  **$\beta 53-12SB_2$** ,  **$\beta 53-12SB_3$** ,  **$\beta 53-8SB_3$** ) were taken up with efficiencies that equal or exceed that of (**PRR**)<sub>3</sub><sup>Flu</sup> ( $MCF = 139 \pm 7.48$ ,  $142 \pm 3.45$ , and  $282 \pm 21.4$  respectively). Uptake in this system appears to depend more on total charge than side chain identity, as  **$\beta 53-12SB_2$** <sup>Flu</sup> was taken up as efficiently as the ornithine-containing analogue  **$\beta 53-12$** <sup>Flu</sup>,<sup>[20]</sup> but less efficiently than  **$\beta 53-12SB_3$** <sup>Flu</sup> and  **$\beta 53-3SB_3$** <sup>Flu</sup>, which each contain three arginines on the salt bridge face.  **$\beta 53-12R_6-1$** <sup>Flu</sup> and  **$\beta 53-12R_6-2$** <sup>Flu</sup> were taken up more efficiently than  **$\beta 53-12$** <sup>Flu</sup> but were not pursued because of their low affinity for hDM2. As expected,  $\beta^3$ -peptides with an  $\alpha$ -arginine tag were taken up well ( $MCF = 10700 \pm 1060$  for  **$\beta 53-12R_8$** <sup>Flu</sup> and  $2670 \pm 52.5$  for  **$\beta 53-3R_8$** <sup>Flu</sup>). Unlike the  $\alpha$ -peptide controls, all of the  $\beta^3$ -peptides that were studied demonstrated increased uptake at a longer time-point (4 h); this highlights their resistance to degradation (see the Supporting Information). The relative cytotoxicities of cell-permeable  $\beta^3$ -peptides were assessed using a commercially available cell viability assay (CellTiter-Blue™, Promega).  **$\beta 53-12$**  and  **$\beta 53-12SB_2$**  were minimally toxic even at  $10 \mu M$ , the concentration used to monitor cell uptake (Figure 4), whereas  $\beta^3$ -peptides containing three or more  $\beta^3$ hR reduced HCT116 cell viability below 80% at this concentration. The toxicity of these latter peptides was even more pronounced at a concentration of  $30 \mu M$  (Supporting Information).

Although a trypsin wash was included in the flow cytometry protocol to remove cell surface proteins that might sequester  $\beta^3$ -peptide,<sup>[21]</sup> confocal microscopy was used to confirm internalization and evaluate the subcellular location of  $\beta^3$ -peptides taken up by HCT116 cells. All of the cell-penetrating peptides

that bound hDM2 ( **$\beta 53-12$** ,  **$\beta 53-12SB_2$** , and  **$\beta 53-12SB_3$** ) showed punctate intracellular fluorescence that co-localizes with 10 kDa dextran, suggesting that  $\beta^3$ -peptide entry proceeds through a form of endocytosis (Figure 5).

Finally, we performed preliminary experiments to assess whether the cell permeability of  $\beta^3$ -peptides  **$\beta 53-12SB_2$** ,  **$\beta 53-12SB_3$** , and  **$\beta 53-12R_8$**  was sufficient to measurably antagonize p53/hDM2 complexation in live cells. HCT116 cells were treated with each of these three  $\beta^3$ -peptides for 8 h along with the control  **$\beta 53-12$** ,<sup>[16]</sup> and the lysates probed for p53, hDM2, and p21 using Western blots. Previous work has shown that p53/hDM2 antagonists stabilize p53 levels and induce expression of the p53 target genes hDM2 and p21.<sup>[22]</sup> As shown in Figure 6, both  **$\beta 53-12$**  and  **$\beta 53-12SB_2$**  increase the levels of p53, albeit modestly, and increase the levels of hDM2 and p21 by approximately two-fold. Both  **$\beta 53-12SB_3$**  and  **$\beta 53-12R_8$**  were too cytotoxic at these concentrations to achieve reliable results. While it is certain that further experimentation<sup>[23]</sup> is necessary to identify the optimal balance between  $\beta^3$ -peptide sequence, hDM2 affinity, cell permeability, and toxicity, these

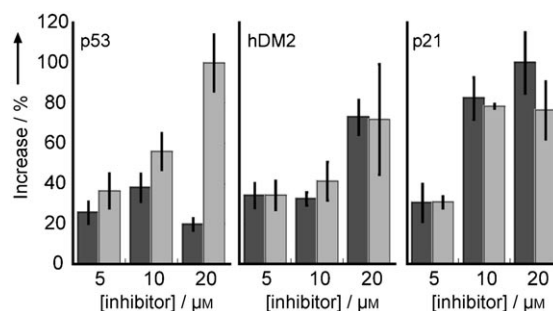


**Figure 6.** Quantification from Western blot analysis of the effects of  **$\beta 53-12$**  (dark gray) and  **$\beta 53-12SB_2$**  (light gray) on p53, hDM2, and p21 levels in HCT116 cells. Original blots in the Supporting Information. Chemiluminescent signal was quantified based on pixel intensity using ImageQuaNT™ software. Bar graphs show the percent increase in pixel intensity over control cells without any  $\beta^3$ -peptide added (all normalized to GAPDH loading control). Each value represents the average of three independent trials. Error bars represent the standard error.

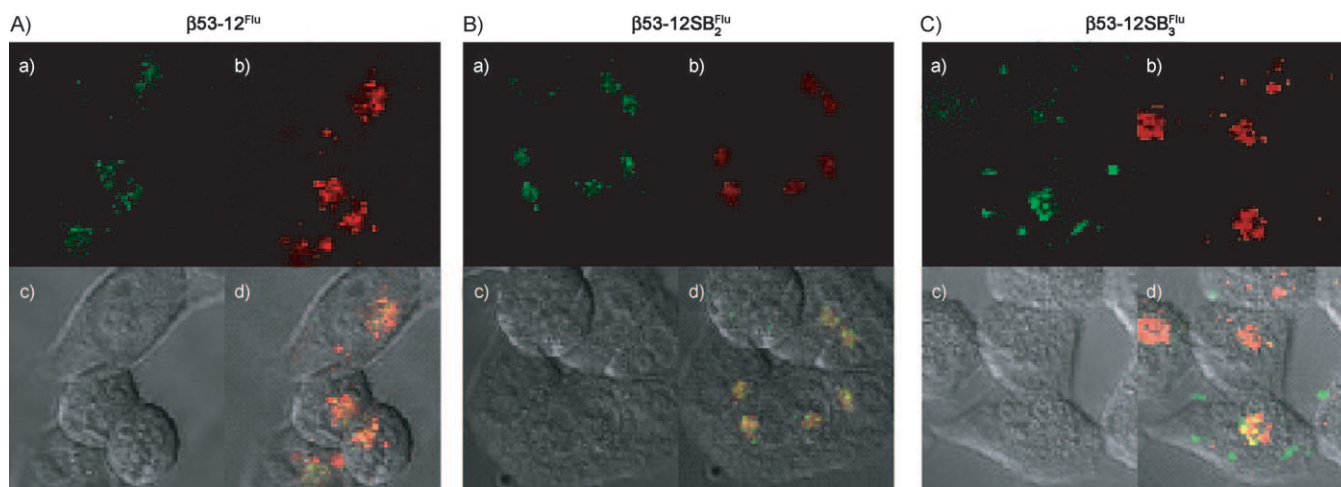


**Figure 5.** Confocal microscopy analysis of HCT116 cells treated with  $\beta^3$ -peptides A)  **$\beta 53-12$** <sup>Flu</sup>, B)  **$\beta 53-12SB_2$** <sup>Flu</sup>, C)  **$\beta 53-12SB_3$** <sup>Flu</sup>. HCT116 cells were incubated with  $20 \mu M$  fluorescein-labeled  $\beta^3$ -peptide (green) for 2 h. Endosomes were visualized using  $10 \mu M$  10 kDa dextran labeled with AlexaFluor™ 647 (red). a) Signal from  $\beta^3$ -peptide only, b) signal from dextran only, c) bright-field only, d) two-color fluorescence with bright-field superposition.

preliminary results indicate that the minimally cationic  $\beta^3$ -peptides reported herein represent the critical first step towards a class of protease-resistant peptidomimetics that fulfill the promise of  $\beta^3$ -peptides as modulators of intracellular biological pathways.

## Experimental Section

**General:** All  $\beta^3$ -peptides were synthesized on a 25  $\mu\text{M}$  scale using standard solid-phase Fmoc chemistry, tagged on the N-terminus when necessary, and purified by reverse-phase HPLC as previously described.<sup>[16]</sup> Fmoc- $\beta^3$ -(L)-amino acids were synthesized from enantiomerically pure  $\alpha$ -amino acids by using the Arndt–Eistert procedure<sup>[11]</sup> with the exception of Fmoc-(S)-3-amino-4-(3-trifluoromethylphenyl)butyric acid and Fmoc-(S,S)-trans-2-aminocyclohexane-1-carboxylic acid, which were purchased from AnaSpec, Inc. (San Jose, CA, USA). For characterization of novel  $\beta^3$ -peptides used in this study, please see the Supporting Information. Protein overexpression and fluorescence polarization assays were performed as previously described.<sup>[4,16]</sup> Circular dichroism was performed using a Jasco J-810 spectropolarimeter.

**Flow cytometry:** HCT116 cells (American Type Culture Collection, Manassas, VA, USA) were grown in T-75 culture flasks containing McCoy's 5 A Medium supplemented with fetal bovine serum (10%) to ~80% confluency, washed twice with 37 °C PBS and incubated with 37 °C PBS-based nonenzymatic cell dissociation solution (10 mL, Chemicon International, Temecula, CA, USA) for 15 min. Cells were centrifuged at 500 g, resuspended in media, counted by hemocytometer, and diluted to 2200 cells per  $\mu\text{L}$  with media. Aliquots of cells (230  $\mu\text{L}$ ) were added to fluorescein-labeled peptides (20  $\mu\text{L}$ , 125  $\mu\text{M}$  in PBS). Cells were incubated with peptide for 1–4 h at 37 °C and then washed twice with 37 °C PBS (750  $\mu\text{L}$ ) to remove extracellular peptide. To ensure removal of any surface-bound peptide,<sup>[21]</sup> cells were then incubated with trypsin (0.25%, 500  $\mu\text{L}$ ) at 37 °C for 10 min, washed once with 4 °C media and once with 4 °C PBS (750  $\mu\text{L}$  each). Cells were suspended in PBS (500  $\mu\text{L}$ ) with propidium iodide (1  $\mu\text{g mL}^{-1}$ ) and analyzed on a BD FACScan (BD Biosciences, San Jose, CA) equipped with a 488 nm Argon laser. A total of 10000 events were collected monitoring fluorescein and propidium iodide with 530/30 bandpass and 650 longpass filters, respectively. Events corresponding to cellular debris were removed by gating on forward and side scatter, while dead cells were removed by propidium iodide staining. Geometric means were then calculated from the histogram of fluorescence intensity and corrected for background cellular fluorescence by subtracting the geometric mean of cells treated only with PBS.

**Confocal microscopy:** HCT116 cells (ca.  $10^5$  per well) were seeded in 6-well plates containing media (2 mL) and cover glasses. After allowing the cells to adhere for 48 h, media was removed by aspiration and the cells were washed twice with 37 °C PBS. Inverted cover glasses were floated on media containing peptide labeled with fluorescein (200  $\mu\text{L}$ , 20  $\mu\text{M}$ ) and/or 10 kDa dextran labeled with AlexaFluor 647 (200  $\mu\text{L}$ , 10  $\mu\text{M}$ , Invitrogen) for 2 h at 37 °C. Cover glasses were then washed with 37 °C media and PBS and mounted on microscope slides. Cells were imaged on an LSM 510 Meta (Carl Zeiss Microimaging, Thornwood, NY, USA) using a 488 nm Ar laser line with a 525/25 nm filter or 633 nm HeNe laser line with a 680/30 nm filter for visualizing fluorescein and AlexaFluor 647, respectively.

**Cellular viability assays:** HCT116 cells (5000/well) were seeded in 96-well plates and allowed to adhere for at least 24 h prior to the

addition of nonfluorescent  $\beta^3$ -peptides (solutions prepared in water). After 8 h incubation with the  $\beta^3$ -peptides at 37 °C, CellTiter Blue® reagent was added and cells were incubated for another 2 h at 37 °C. The reduction of rezazurin to resorufin was monitored by fluorescence using an Analyst™ AD 96–384 fluorescence plate reader (LJL Biosystems, Sunnyvale, CA) using 530/25 excitation and 580/10 emission filters. Cell viability was calculated as the percentage of signal from the  $\beta^3$ -peptide-treated cells compared to water-treated cells. The mean viability with standard error of three independent experiments, each containing at least three replicates, is reported.

## Acknowledgements

This work was supported by the National Institutes of Health (GM 74756) and the National Foundation for Cancer Research. The authors also thank Alston Wendlandt and James Nelson for assistance with  $\beta^3$ -peptide synthesis and purification.

**Keywords:** beta-peptides • hDM2 • inhibitors • p53 • peptidomimetics

- [1] D. Seebach, M. Overhand, F. N. M. Kuhnle, B. Martinoni, L. Oberer, U. Hommel, H. Widmer, *Helv. Chim. Acta* **1996**, *79*, 913–941.
- [2] R. P. Cheng, S. H. Gellman, W. F. DeGrado, *Chem. Rev.* **2001**, *101*, 3219–3232.
- [3] K. Gademann, T. Kimmerlin, D. Hoyer, D. Seebach, *J. Med. Chem.* **2001**, *44*, 2460–2468.
- [4] J. A. Kritzer, J. D. Lear, M. E. Hodsdon, A. Schepartz, *J. Am. Chem. Soc.* **2004**, *126*, 9468–9469.
- [5] J. A. Kritzer, N. W. Luedtke, E. A. Harker, A. Schepartz, *J. Am. Chem. Soc.* **2005**, *127*, 14584–14585.
- [6] J. Frackenkohl, P. I. Arvidsson, J. V. Schreiber, D. Seebach, *ChemBioChem* **2001**, *2*, 445–455.
- [7] C.-H. Tung, R. Weissleder, *Adv. Drug Delivery Rev.* **2003**, *55*, 281–294.
- [8] S. W. Jones, R. Christison, K. Bundell, C. J. Joyce, S. M. V. Brockbank, P. Newham, M. A. Lindsay, *Br. J. Pharmacol.* **2005**, *145*, 1093–1102.
- [9] S. M. Fuchs, R. T. Raines, *Protein Sci.* **2005**, *14*, 1538–1544.
- [10] N. J. Zondlo, A. Schepartz, *J. Am. Chem. Soc.* **1999**, *121*, 6938–6939.
- [11] J. W. Chin, A. Schepartz, *J. Am. Chem. Soc.* **2001**, *123*, 2929–2930.
- [12] D. S. Daniels, A. Schepartz, *J. Am. Chem. Soc.* **2007**, *129*, 14578–14579.
- [13] M. Rueping, Y. R. Mahajan, M. Sauer, D. Seebach, *ChemBioChem* **2002**, *3*, 257–259.
- [14] N. Umezawa, M. A. Gelman, M. C. Haigis, R. T. Raines, S. H. Gellman, *J. Am. Chem. Soc.* **2002**, *124*, 368–369.
- [15] T. B. Potocky, A. K. Menon, S. H. Gellman, *J. Am. Chem. Soc.* **2005**, *127*, 3686–3687.
- [16] E. A. Harker, D. S. Daniels, D. A. Guarracino, A. Schepartz, *Bioorg. Med. Chem.*; in press.
- [17] E. A. Harker, A. Schepartz, *unpublished results*.
- [18] W. F. DeGrado, J. P. Schneider, Y. Hamuro, *J. Pept. Res.* **1999**, *54*, 206–217.
- [19] E. Vives, P. Brodin, B. Lebleu, *J. Biol. Chem.* **1997**, *272*, 16010–16017.
- [20] D. J. Mitchell, D. T. Kim, L. Steinman, C. G. Fathman, J. B. Rothbard, *J. Pept. Res.* **2000**, *56*, 318–325.
- [21] J. P. Richard, K. Melikov, E. Vives, C. Ramos, B. Verbeure, M. J. Gait, L. V. Chernomordik, B. Lebleu, *J. Biol. Chem.* **2003**, *278*, 585–590.
- [22] A. Bottger, V. Bottger, A. Sparks, W.-L. Liu, S. F. Howard, D. P. Lane, *Curr. Biol.* **1997**, *7*, 860–869.
- [23] P. Yu, B. Liu, T. Kodadek, *Nat. Biotechnol.* **2005**, *23*, 746–751.

Received: January 29, 2009

Published online on March 5, 2009